

N85-32744

Microanalysis of Dissolved Iron and Phosphate in Pore Waters of Hypersaline Sediment

R. Haddad and T. Shaw

Introduction

Reduced iron, soluble in acidic pH, has an intermediate redox potential; it may serve as an intermediate electron acceptor-donor between O_2 and S^{2-} . Furthermore, reduced iron is abundant in many fresh water and marine sediments. Iron may serve as an alternative electron donor in cyanobacterial photosynthesis (Cohen, personal communication).

Diurnal fluctuations of reduced iron concentrations, expected to occur in reduced sediments in the photic zone, were studied. Iron concentration was compared to O_2-H_2S , a microanalysis of sulfate reduction was performed, as well as an examination of diurnal concentration of dissolved phosphate and changes in interstitial CO_2 .

Materials and Methods

Pore Water Iron Determination

Dissolved iron concentrations in sediment pore waters were determined colorimetrically by the ferrozine method (Stookey, 1970, modified by Murray and Gill, 1978). Further modifications of the original method were necessary to work with the limited sample size (0.5 ml) used with the millimeter pore water method described in the following section. A small amount (0.3 ml) of sample was added to 0.1 ml of ferrozine reagent, 0.1 ml hydroxylamine hydrochloride, and 1 ml of MilliQ purified water. The solution reacted for 10 minutes in an 80°C water bath. The samples were allowed to cool to room temperature and 0.1 ml of ammonium acetate buffer was added. The absorption of the resulting iron complex was measured at 562 nanometers in a 0.5 ml microcell. A standard curve and blank were measured with each set of pore water profiles.

Phosphate Assays

Dissolved phosphate concentrations in pore waters were determined colorimetrically by the stannous chloride method. Several modifications to the method were adopted to allow determination using 0.1 ml of sample. An acidic solution consisting of 0.1 ml of concentrated KCl in 100 ml of distilled water was used to dilute the pore water sample. The stannous chloride solution was diluted 1:5 with ethanol to allow more accurate addition of solution. To 1 ml of acidic solution were added 0.1 ml of sample, 0.02 ml of molybdate reagent, and 0.03 ml of stannous chloride solution. After ten minutes the absorption of the solution was measured at 690 nm.

Carbon Isotope Ratio Determination Methods

Sampling Procedure

3 to 5 cm-long sediment cores were collected using 1 1.2 cm diameter acrylic core tubes. These core tubes were specially designed; one end was tapered for easier sediment penetration and the other end was faced off for precise sectioning. The cores were returned to the San Jose State University laboratories within three hours of collection and incubation processes begun immediately.

Extruding Procedure

For sum CO₂ and ferrous iron analyses, the cores were transferred into a nitrogen atmosphere glove bag for processing. Procedural blanks indicated that the carbon dioxide concentration within the glove bag was less than 0.6 nM. Inside the glove bag, cores were extruded and sectioned into 1 mm or 2 mm sections using a .036 cm glass reinforced epoxy sheet. The error was estimated to be 1 mm plus or minus 0.5 mm sections. Pore water was obtained via ultracentrifugation for 10 minutes of the sliced sections, transferred and centrifuged a second time to insure particulate removal.

Total Carbon Dioxide Pore Water Procedure

A known volume of the particulate free pore water was transferred by syringe from the centrifuge tubes into 15.75 ml Pierce crimp-top vials. These were immediately crimped using septa and tear-away aluminum crimp tops. The stoppered vials were removed from the glove bag and stored at -76 degrees centigrade until isotopic analyses could be done (0.5-1 day).

Vacuum Line Procedures

Prior to isotopic analysis, the frozen pore water samples were allowed to equilibrate to ambient room temperature (approximately 25 °C). Two ml of 1 M sulfuric acid were added to liberate the total carbon dioxide as carbon dioxide gas. A 2 M sulfuric acid plus 2 M cuprous sulfate solution was experimented with in anticipation of high concentrations of sulfide; however, the lack of any CuS precipitate demonstrated that the concentration of hydrogen sulfide in the upper 1 cm of sediment would not interfere with the ¹³C/¹²C isotopic measurements. The CO₂ produced upon acidification was purified, isolated, measured for volume, and collected using vacuum line techniques in Dr. David DesMarais' carbon isotope laboratory at the NASA Ames Research Center (see PBME, 1982, NASA Technical Memorandum 86043 for details).

Stable Isotope Mass Spectrometer Procedure

$^{13}\text{C}/^{12}\text{C}$ isotopic measurements were made on a 6" nuclide stable isotope mass spectrometer and are presented in the usual δ notation referenced to the Pee Dee belemnite (PDB) standard (See Table I-2 p).

Paratetramitus and Manganese-Oxidizing Bacteria

For methods see Read, et al, 1983. Manganese acetate plates were inoculated in the center with 1 mm³ of sediment sample and flooded with 1 ml distilled water for each 1 mm depth for the 42 per mil site.

Results

Pore water from the upper centimeter of the 42 per mil pond was analyzed to determine the concentrations of dissolved iron and phosphate. The iron profiles suggest a strong correlation between iron remobilization and processes occurring in the light (see Fig. IV-13). Phosphate profiles (Fig. IV-14) suggest the removal of phosphate is strongly correlated with precipitation of oxidized iron in the upper 2-5 mm of the sediments. Phosphate concentrations were higher in the dark cycle cores where the iron diffusion gradient to the oxidized zone of the sediment is at a minimum. Although phosphate removal is associated with iron removal, there is little evidence for phosphate remobilization associated with iron remobilization. Phosphate appears to diffuse upward from below. This observation suggests that the mechanism of iron remobilization during the light cycle does not involve reduction of oxidized iron. Further, the correlation of iron remobilization with light cycle processes suggest that the mechanism of iron mobilization may be the result of an oxidative process.

Pore water ΣCO_2 concentrations and carbon isotope ratios are presented (Figure IV-15 and IV-17). These data are from the analyses of mini-sediment cores collected from the 42 per mil salt pond and incubated in the laboratory under light and dark conditions. The $\delta^{13}\text{C}$ values in the light-incubated core decrease from -5.24 - 0.19 per mil at 0-1 mm to -7.89 per mil at 1-3 mm and increase back to about -6 per mil at 6-10 mm. When sampling resolution is decreased to 2 mm intervals (Figures IV-15, 16, and 17) the major down core trends of heavy CO_2 at the surface are still evident but the fine-scale structure of the profile changes.

The large difference between the $\delta^{13}\text{C}$ values in the 0-1 and 1-2 mm sections measured in the light-incubated cores is not present in the dark-incubated cores. In these cores, the isotope values are fairly constant over the upper 5 mm; they increase from 5-7 mm and level off in the 7-10 mm region.

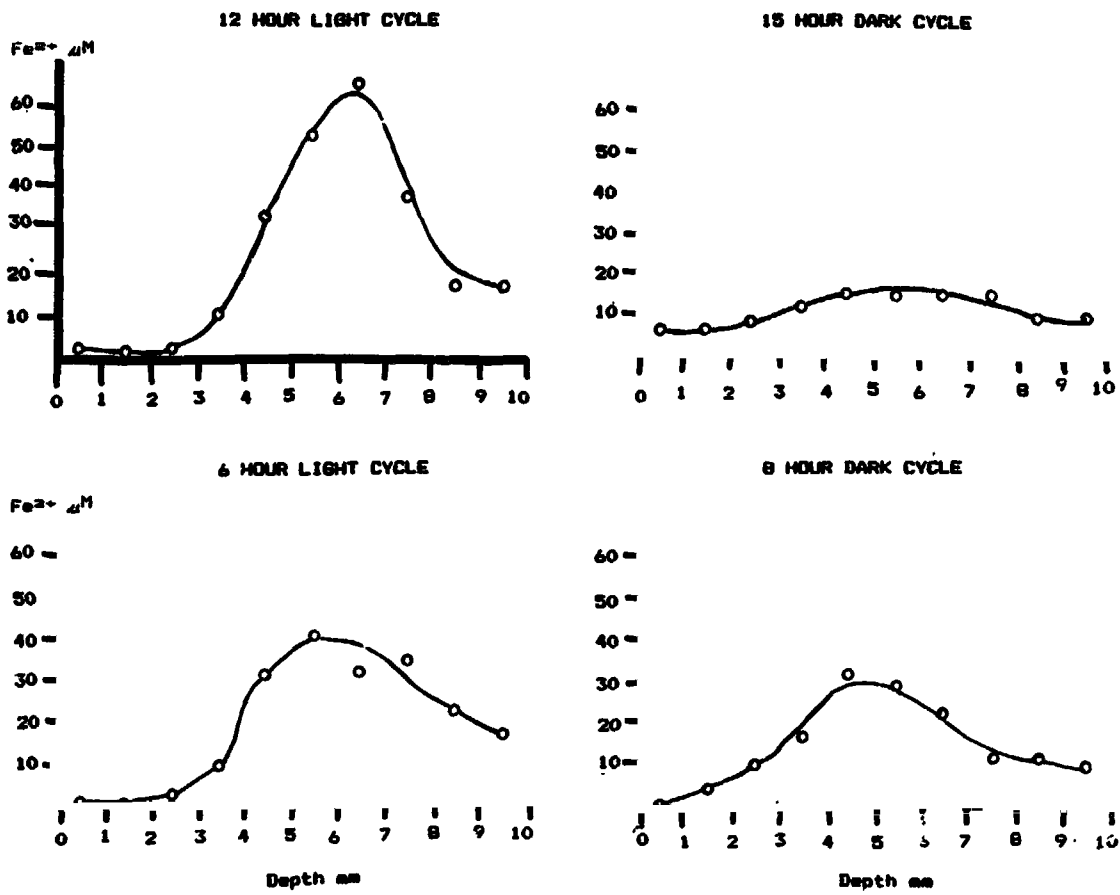


Figure IV-13. Iron profiles (42 per mil pond).

ORIGINAL PAGE IS
OF POOR QUALITY

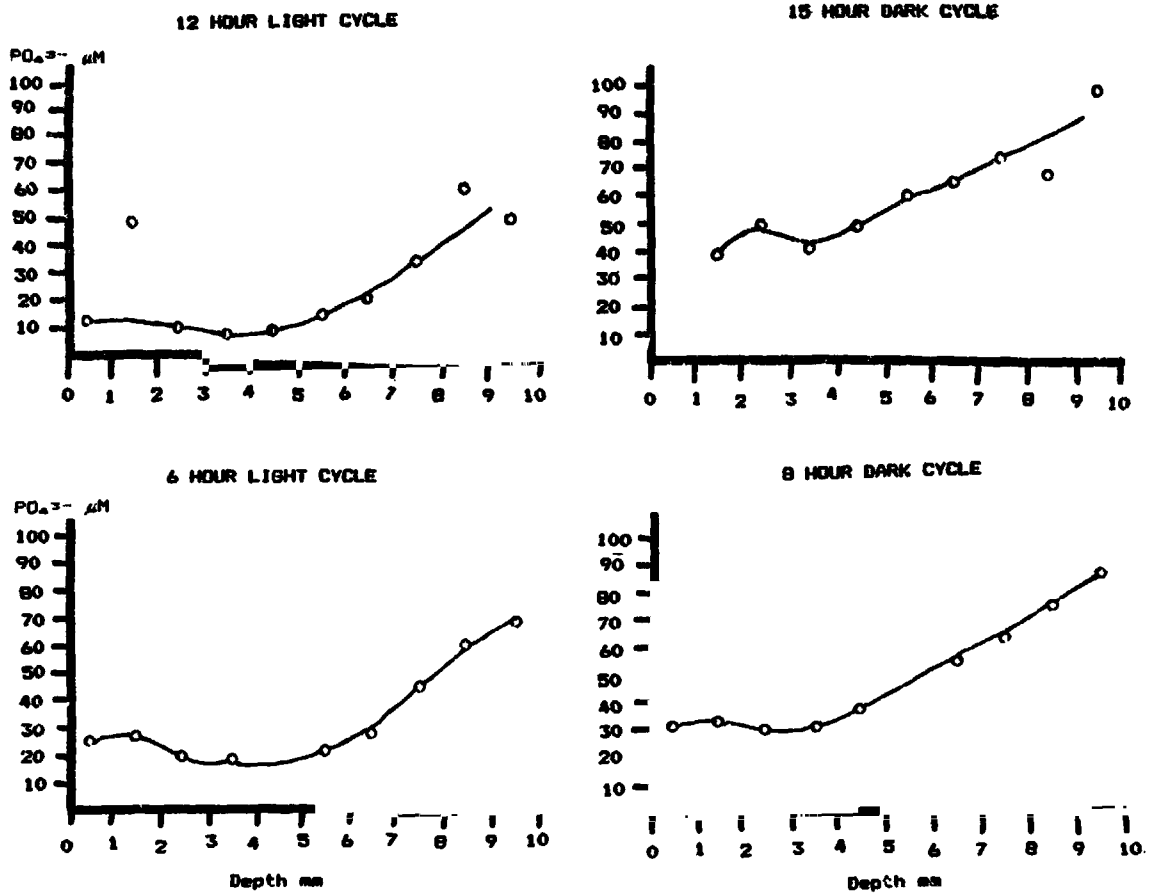
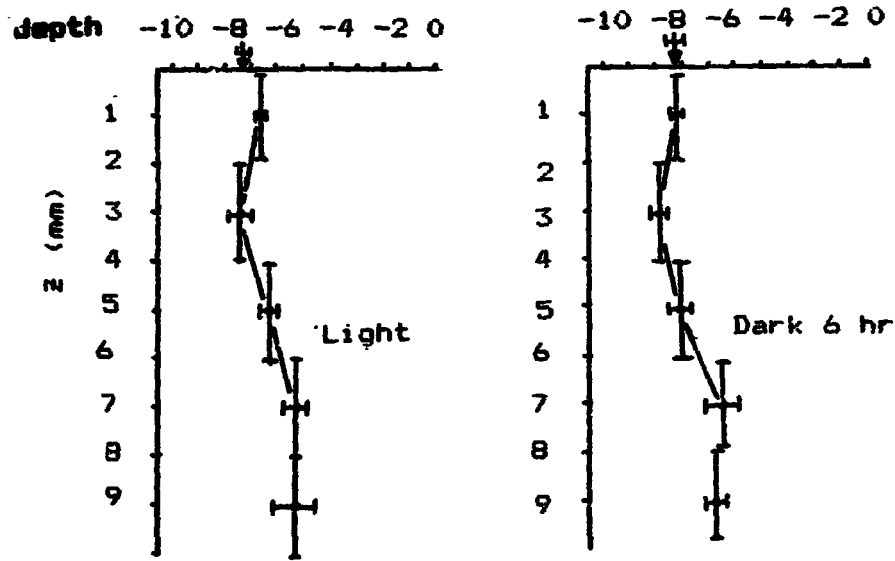
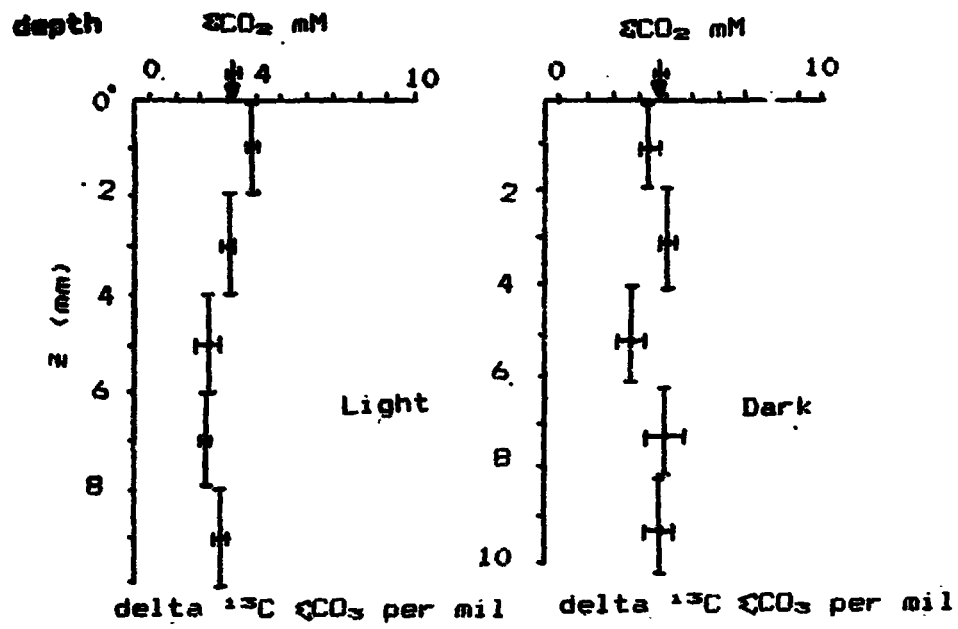


Figure IV-14. Phosphate profiles (42 per mil pond).



ORIGINAL PAGE IS
OF POOR QUALITY

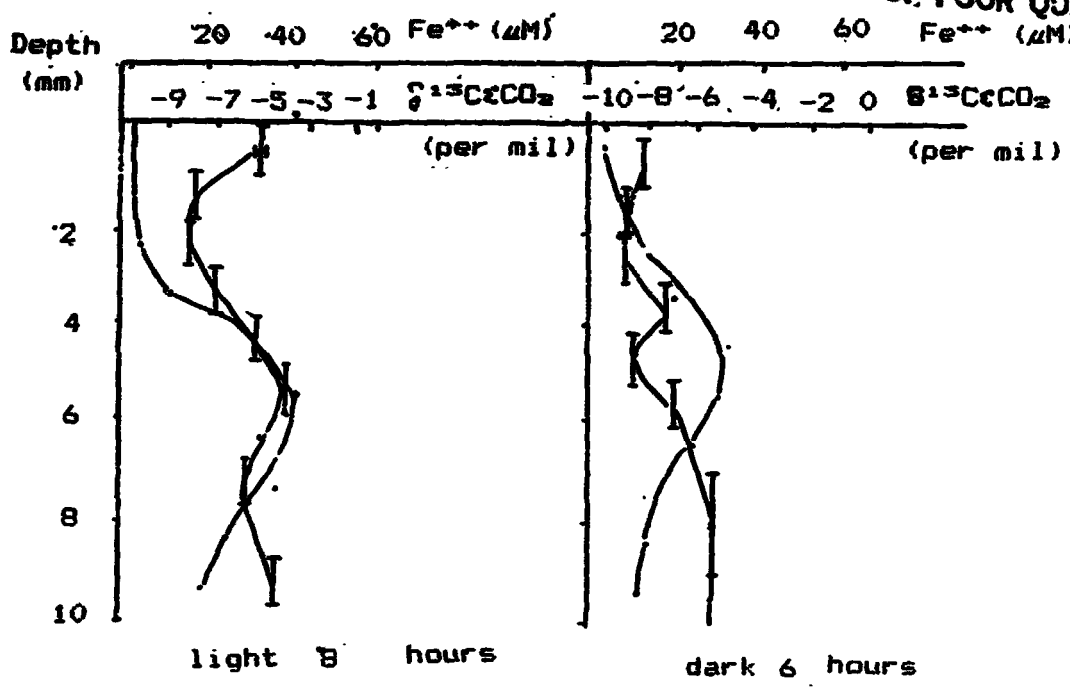


Figure IV-15. Comparison of concentration of dissolved Fe⁺⁺ and delta ¹³CO₂ in the interstitial water.

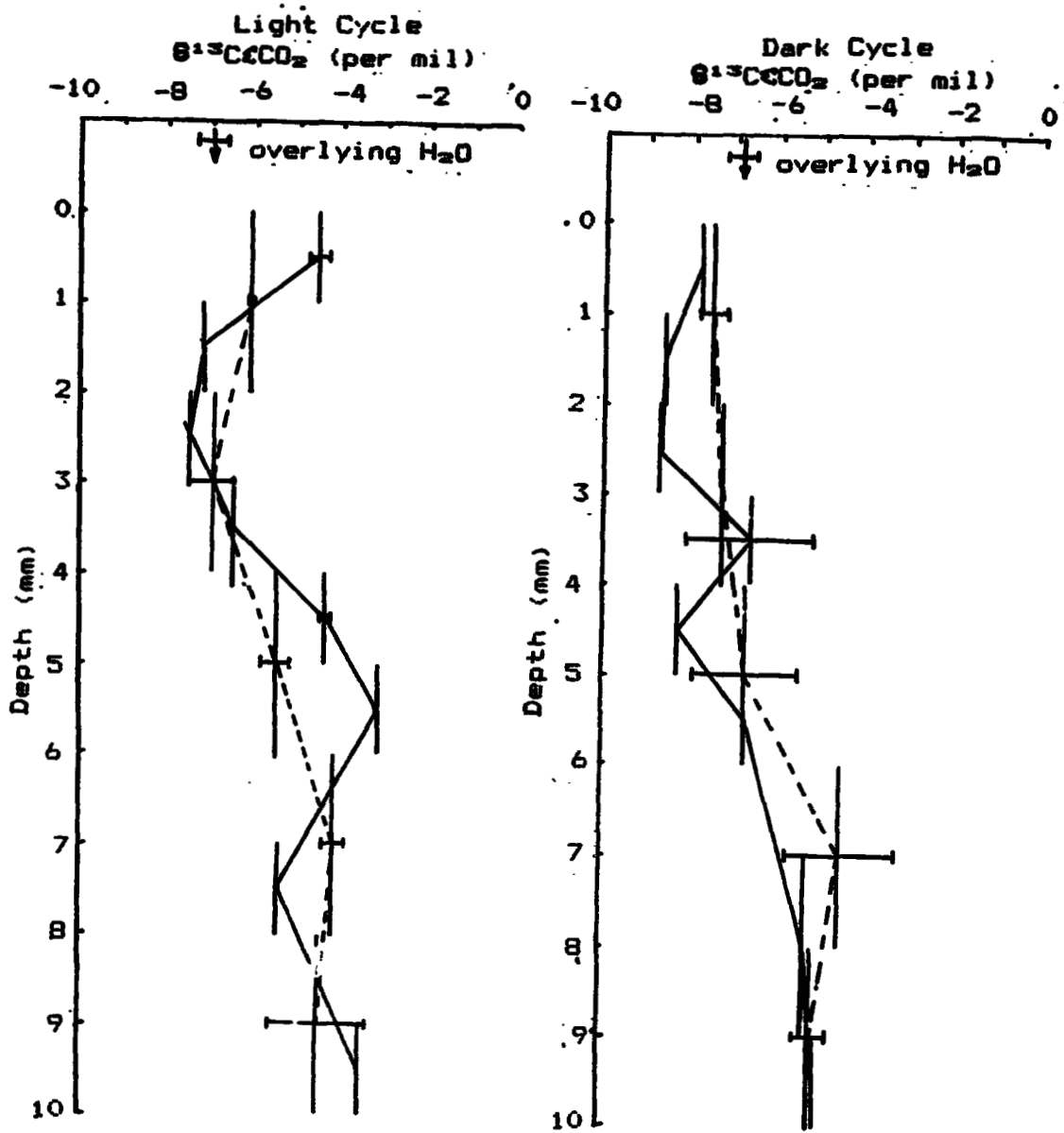


Figure IV-16. Light cycle delta $^{13}\text{C}(\text{CO}_2)$ profile.

Figure IV-17. Dark cycle delta $^{13}\text{C}(\text{CO}_2)$ profile.

The ΣCO_2 pore water concentrations are presented for the 2 mm sectioned cores only in Figure IV-15. In the light-incubated core, there is a gradual decrease in ΣCO_2 concentrations from 3.89 ± 0.14 mM at 0-2 mm to 2.11 ± 0.43 mM at 7-8 mm. No such trend is evident in the ΣCO_2 concentration profile in the dark-incubated core. In this core, CO_2 ranges from 2.74 ± 0.86 mM to 4.08 ± 0.37 mM.

Colonies of manganese-oxidizing bacteria appeared in all samples studied. Millimeter samples showed the most activity for both *Paratetrasitus* and manganese oxidizers at 6 millimeters below the surface (Table IV-4).

Discussion

Partial oxidation of sulfide in the form of iron monosulfide may explain these iron profiles. The presence of elemental sulfur in the upper centimeter of these sediments (Chapter III) confirms the assumption that the sulfide is being oxidized in this zone but the presence of dissolved iron to depths of 8-9 millimeters suggests that very little free sulfide is available for oxidation in this zone.

An important aspect of the proposed mechanism is that iron monosulfide in the presence of elemental sulfur reacts to form pyrite, the ultimate sulfur sink in the sediments; these two reactants, however, are not usually found in the same sedimentary regime. The mechanism suggests that in this environment elemental sulfur and iron monosulfide can exist concurrently. Furthermore, rates of pyrite formation in these sediments are greatest in the top centimeter (see Chapter III).

Recent studies on microbial mat communities using microelectrodes have demonstrated that large gradients in oxygen (0-200 μM), sulfide (0-200 μM) and pH (1-9) exist within the upper 1-3 mm of the mat (Jorgensen et al., 1983). These profiles have been shown to be supported by microbially mediated processes (e.g., photosynthetic CO_2 fixation, CO_2 respiration, sulfate reduction, etc.) and they exhibit diurnal variations. One interesting observation from these studies is that both oxygen and sulfide coexist in low concentrations (200 μM and 50-100 μM respectively) in a narrow zone within the upper few mm of the mats. This chemical boundary is usually exploited by sulfur-oxidizing bacteria such as *Beggiatoa* and flexibacteria yet results from recent experiments using a new ^{35}S -sulfate reduction determination technique qualitatively demonstrate that sulfate reduction is occurring in this microaerophilic environment at significant rates (Y. Cohen, personal communication). In this microenvironment, photosynthetic products (amino acids, short-chained fatty acids, etc.) excreted by the phototrophic bacteria may be utilized as carbon sources by sulfate-reducing bacteria. Microbially-mediated degradation processes such as sulfate reduction and fermentation are assumed to be primarily by organic

matter produced *in situ* in the mat communities.

The results of the O₂ and sulfide profiles and pore water Σ CO₂ concentrations and carbon isotopic values do not support this hypothesis. Instead they argue that organic matter from the overlying water column limits degradative processes. During the light cycle, oxygen is present only in the upper 1-2 mm where active photosynthesis occurs. Concurrently, sulfide does not appear to be present in the pore water until 6-8 mm depth and even then only in trace quantities (less than 0.1 mM). During the dark period, oxygen is present in much lower concentrations, and sulfide apparently is present in trace amounts up to the sediment/water interface.

A comparison of the light and dark Σ CO₂ carbon isotope profiles (Fig IV-15) demonstrates a significant diurnal variation in the upper 1-2 mm due to the photosynthetic activity. During the light cycle, relatively light carbon dioxide (carbon dioxide enriched in ¹²C with respect to ¹³C) is fixed, thereby enriching the remaining sum carbon dioxide pool in ¹³carbon dioxide with respect to ¹²carbon dioxide. This results in an increase in the delta ¹³C value. During the dark cycle, carbon dioxide is not fixed and respiration by heterotrophs produces light carbon dioxide thereby decreasing the delta ¹³C sum carbon dioxide value in the pore water.

Directly below the photosynthetic zone, the proposed coupling of sulfate reduction with photosynthetic activity should result in lighter delta ¹³C Σ CO₂ values in the pore water during the light cycle (when the light - roughly 30 per mil - photosynthate is being produced). The light/dark profiles demonstrate that the pore water delta ¹³C CO₂ is actually lighter during the dark cycle presumably due to heterotrophic (fermentative) activity, and the absence of photosynthetic activity.

These isotopic data suggest that the degradation processes mediated by microbes are driven not by *in situ* photosynthetically derived organic matter, but by allochthonous organic matter (presumably from the overlying water column). This view is supported by the Σ CO₂ and delta ¹³C values in the overlying water column. Comparing the measured values with predicted values based on concentrating seawater to 42 per mil, the measured Σ CO₂ concentration values range from 10-25 percent greater than the predicted values. Also, the delta ¹³C values in the water column are 5-7 per mil lighter than the predicted value of about 0 per mil. In addition, there appears to be a net export of Σ CO₂ from the sediment to the overlying water column, completing a type of mini-carbon cycle which, for the most part, bypasses the processes of sedimentary CO₂ fixation.

A final curiosity is the increase in the ΣCO_2 delta ^{13}C profile in the 6-8 mm interval in which no diurnal variation is seen. These isotope values may be indicative of some type of chemoautotrophic CO_2 fixation. Although this would explain the heavy shift in isotope, no significant concentration change is seen. There appears to be a slight decrease in ΣCO_2 concentration in the dark profile; the precision of the light profile is such that no trend is clear. If these isotope profiles are superimposed upon those of the dissolved ferrous iron it can be seen that the maximum pore water ferrous iron concentration occurs in a zone where chemoautotrophic uptake of CO_2 is proposed. This maximal zone (6-7 mm in the light) seems to support the highest concentration of manganese-oxidizing bacteria and their predators, *P. jugosus* (an amoebomastigote, Table IV-5).

In summary, the ΣCO_2 , isotope, and concentration profiles measured in a mm interval demonstrate that the upper 1 cm of this environment is extremely dynamic. There appears to be no direct relation between photosynthesis occurring in the mat community and microbially mediated degradation processes. Rather, the sedimentary microbial processes appear to be driven by allochthonous organic matter. The ΣCO_2 concentration and isotopic composition reflect microbially mediated degradation processes occurring within the sediment. In conclusion, we propose that the upper 10 mm of this environment can be viewed as having three geochemically distinct zones: 1) the upper 0-2 mm dominated by the diurnal variations in photosynthesis, 2) a middle 2-4 mm zone dominated by heterotrophic activity, and 3) a deeper 4-10 mm zone in which some chemoautotrophic activity is occurring together with ferrous iron and phosphate geochemical reactions.